Seismic Fragility Assessment of Unreinforced Masonry Shear Walls

Jayaprakash Vemuri and K. V. L. Subramaniam

1 Introduction

The Kutch region in the western part of India is seismically active and has been struck by destructive earthquakes in the past. The M_w 7.6 earthquake which struck Kutch on 26 January 2001 was the largest intraplate earthquake to strike in India [1]. Post-earthquake damage surveys reported intensity levels up to X on the Modified Mercalli Intensity (MMI) scale [2]. The epicentre lay about 9 km southwest of the village of Chobari in the Kutch district of Gujarat, India [3]. The earthquake caused widespread damage in the province of Gujarat. Overall, over a million structures were damaged, and the consequent economic loss was close to US$10 billion [4]. In the Kutch region, the earthquake destroyed several towns causing major devastation of low-rise unreinforced masonry (URM) structures [5]. Typically, URM structures in the region consist of load-bearing masonry shear walls made of low-strength bricks. The performance of shear walls greatly affects the vulnerability of masonry buildings, and it is imperative to assess their seismic fragility.

In India, 69% of buildings are constructed using unreinforced brick masonry [6]. However, barring a few classical studies [7, 8] the in-plane behaviour of URM walls has not received much attention [9, 10]. The research reported varies widely due to inconsistency in test practices [11]. While researchers have conducted nonlinear time-history analyses of URM structures, there is no available literature presenting the correlation between ground motion parameters and URM structural response. Also, the lack of recorded seismic data from major earthquakes of the Kutch region presents a major challenge to the seismic assessment. Even the available information

J. Vemuri (✉)
Mahindra Ecole Centrale, Hyderabad, India
e-mail: jayaprakash.vemuri@mechyd.ac.in

K. V. L. Subramaniam
Indian Institute of Technology Hyderabad, Sangareddy, India
e-mail: kvls@iith.ac.in

K. V. L. Subramaniam and Mohd. A. Khan (eds.), *Advances in Structural Engineering*, Lecture Notes in Civil Engineering 74,
https://doi.org/10.1007/978-981-15-4079-0_1

following the major Kutch earthquake (M_w 7.6 at 8:46 a.m. on 26 January 2001) is limited to recorded peak ground accelerations (PGA) at selected towns. Since the accuracy of seismic assessment depends on capturing the local soil effects, the absence of seismic records from the Kutch region complicates our understanding of the actual seismic hazard.

In this study, ground motions are generated at rock level by the modified stochastic finite-fault method. The PGAs of these synthetic ground motions generated at rock level are compared with bedrock-level PGAs, which are available at thirteen stations. After validation, strong ground motions are generated at surface level by accounting for varied local topography by using site amplification functions for various towns available in the literature [12]. The ground motions are generated at bedrock level and amplified to surface level using the soil amplification functions corresponding to each particular site. The cyclic response of masonry, which is generated using an analytical-based model for the shear response of masonry, is used to investigate the vulnerability of the masonry to different parameters of the ground motions.

2 Material and Geometric Properties of URM Walls

Under lateral forces, a URM wall may fail due to sliding, flexure/rocking or shear. Sliding occurs along bed and head joints under low values of normal stress. Masonry can also crack under direct tension. Walls with high aspect ratios typically exhibit flexural or rocking behaviour while those with moderate aspect ratios fail in shear. In shear failures of URM walls, pre-cracking behaviour is characterised by mild hysteresis. Flexural cracks originate first, and then diagonal cracks start close to the ultimate shear strength. Diagonal cracking is visible when the peak lateral force is achieved, followed by a degradation in strength. In the post-peak regime, strength and stiffness drop rapidly, and high level of energy is dissipated. The wall collapses by stepped cracking along mortar joints. Cyclic response of the wall is bounded by the monotonic shear–deformation ($V - \Delta$) envelope. To obtain the monotonic envelope for URM walls, an incremental procedure available in the literature [13, 14] is used, where the lateral force is increased in increments, and at each step, the shear and flexural deformations are combined to obtain the load–deformation curve ($V - \Delta$ curve). The flexural strength is computed [7] as:

$$V_r = \frac{pDt}{2\alpha_v}\left(1 - \frac{p}{kf_u}\right) \tag{1}$$

where $p = P/Ht$ is the vertical compressive stress and P is the vertical compressive force. H, D and t represent the height, length and thickness of the wall, f_u is the masonry strength in compression, k is a coefficient which accounts for vertical stress distribution at the compressed toe, $\alpha_v = M/(VD)$ is the shear ratio. The shear strength can be computed [7] as:

$$V_{\mathrm{d}} = Dt\tau_{\mathrm{u}};\ \ \tau_{\mathrm{u}} = \text{minimum}(\tau_{\mathrm{cs}};\ \tau_{\mathrm{ws}};\ \tau_{\mathrm{b}}) \tag{2}$$

τ_{cs} is the shear stress corresponding to the cracked section and is given by:

$$\tau_{\mathrm{cs}} = \frac{1.5c + \mu p}{1 + \frac{3c\alpha_{\mathrm{v}}}{p}} \tag{3}$$

τ_{ws} is the shear stress of the complete section and is given by:

$$\tau_{\mathrm{ws}} = \frac{c + \mu p}{1 + \alpha_{\mathrm{v}}} \tag{4}$$

τ_{b} is the shear stress based on brick cracking and is given by:

$$\tau_{\mathrm{b}} = \frac{f_{\mathrm{bt}}}{2.3}\sqrt{1 + \frac{p}{f_{\mathrm{bt}}}} \tag{5}$$

where c is the joint cohesion, μ is the joint friction coefficient, f_{bt} is the tensile strength of brick. The expressions for joint cohesion and joint friction have been defined [15] as $c' = kc$ and $\mu' = k\mu$ where k is:

$$k = \frac{1}{1 + \mu 2\frac{\Delta_y}{\Delta_x}} \tag{6}$$

where Δ_x and Δ_y are the height and length of the brick unit, respectively. Due to the absence of experimental data on shear walls from India, two shear walls [16, 17] were selected from literature, which are representative of the typical masonry construction in Kutch [18]. Table 1 shows the properties of the two URM walls. The monotonic backbone envelope is computed for both the walls.

The cyclic behaviour was modelled in SAP2000 [19] where the *link element* is chosen to model the URM wall. The multilinear-plastic pivot model is used to define the hysteresis loop. The four pivot parameters, α_1, α_2, β_1 and β_2, govern the shape of the cyclic loops and the degradation in strength and stiffness. The optimum values for the four parameters were obtained using the least-squares method to minimise the error concerning the values obtained from experiments. For the wall with lower axial stress, α_1, β_1, α_2 and β_2 are 0.90. The symmetrical response and no pinching resulted in the parameters to be equal in magnitude. The hysteresis behaviour obtained from the experiment matches well with the loops obtained from the pivot model (Fig. 1a). For the shear wall having higher axial stress, α_1, β_1, α_2 and β_2 were computed to be 0.90. Figure 1b shows the match between the experimental hysteresis loops of the wall and the loops obtained from the pivot model. Limit states corresponding to cracking, ultimate strength and collapse are noted for both walls.

Table 1 Properties of the two URM shear walls considered in the present study

Property	Wall-1	Wall-2
H (mm)	1350	3000
D (mm)	1000	1500
t (mm)	250	380
p (MPa)	0.6	1.24
f_b (MPa)	16	19.7
f_{bt} (MPa)	1.22	1.07
f_m (MPa)	3.31	4.33
f_u (MPa)	6.2	7.9
c (MPa)	0.23	0.21
c' (MPa)	0.17	0.14
μ	0.58	0.81
μ'	0.43	0.55

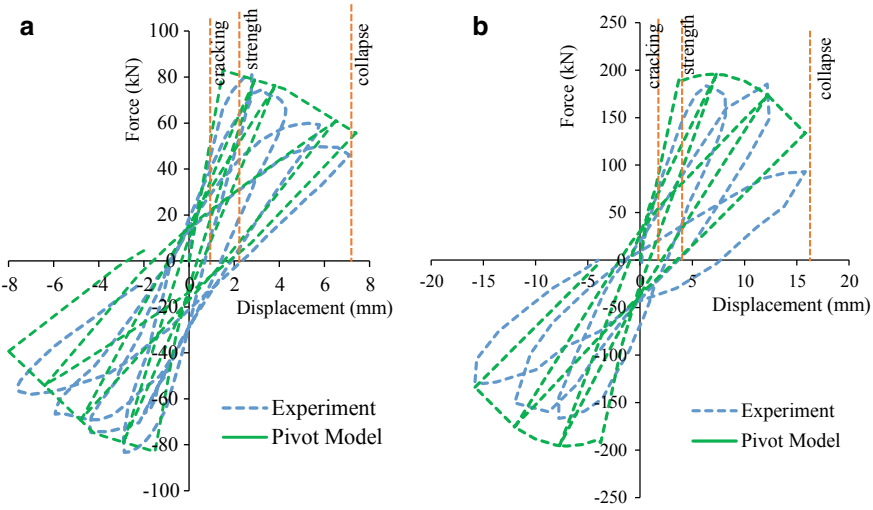

Fig. 1 Comparison between experiment and pivot model. **a** URM wall with diagonal shear cracking through mortar joints; **b** URM wall with shear–tensile cracking of bricks

3 Nonlinear Time-History Analyses Using Synthetic Ground Motions

Seismic records for the 2001 Kutch earthquake are not available. In such regions where a rich database of historical strong motions is unavailable, modified records may be obtained either by generating artificial records or by altering natural records.

The modified stochastic finite-fault method [20] has been used by researchers [21] to generate surface-level synthetic ground motions for the 2001 Kutch earthquake. From these synthetic accelerograms, ground motion characteristics such as PGA, PGV, predominant period, mean period, significant duration and response spectra are computed. Figure 2 shows the ground motions generated at surface level. At each site, ten synthetic ground motions were generated by conducting trials. The modified stochastic finite-fault method is extended to derive synthetic ground motions at surface level, for towns across various seismic zones. These synthetic ground motions are used for nonlinear time-history analyses.

The earthquake hazard in the province of Gujarat ranges from low to high. Based on the estimated hazard level, the seismic zoning map of India IS1893:2016 [22] has assigned four seismic zones to Gujarat, ranging from Zone 2 (low) to Zone 5 (high). The Kutch region has the highest earthquake hazard and lies in Zone 5 (SA at DBE level of 0.45 g), and intensity levels more than IX may be expected in this region. Zone 4 (SA at MCE level of 0.30 g) comprises regions from Saurashtra and Kutch, within a belt with a width of 60–70 km around Zone 5 and intensity VIII may be expected in this zone. Mainland Gujarat is assigned Zone 3 (SA at DBE level of 0.20 g) where intensity level of VII may be expected. Table 2 shows the characteristics of the surface-level synthetic ground motions generated for various towns in Gujarat. These towns are situated across various seismic zones as per the seismic zonation map of India (IS1893:2016). The epicentral distance of the station, the PGA, PGV, the significant duration and, the mean displacements for both walls are tabulated. The MMI data as observed from the earthquake isoseismals [23] to indicate the overall damage to structures in each town is also tabulated in Table 2. Additionally, in this study, two scalar measures, the predominant period, T_p, and the mean period, T_m, were used to assess frequency content in ground motion. Both scalar frequency parameters exhibited a weak correlation with the structural displacements of the two walls. Nevertheless, it is observed that ground motions at most sites exhibited very low predominant periods. From Table 2, it is observed that the mean periods of the ground motions are higher than predominant periods but higher than the natural periods of the walls. Observation of experimental hysteresis loops for wall-1 shows that the stiffness decreased by nine times, causing the fundamental period to increase three times. For wall-2, experimental hysteresis loops indicate that the stiffness decreased by three times. The increased natural period of both walls is close to the frequency content, indicated by T_m, in the ground motion. The low values of both frequency parameters indicate that the seismic energy of the ground motions generated due to the 2001 Kutch earthquake was concentrated in the low time period range. This makes the masonry structures vulnerable to collapse once there is an increase in time period due to damage in the walls.

From Table 2, it is observed that URM walls in Seismic Zone 5 witnessed high displacements which caused collapse. Most ground motions from Zone 5 have PGV values > 0.1 m/s and PGA values > 0.1 g and caused the walls to reach the collapse displacement levels. In Figs. 3 and 4, the PGA and the PGV are correlated with structural displacements of the two walls. The three limit states are marked for reference. Ground motions in the epicentral region, with PGAs > 0.1 g, caused a

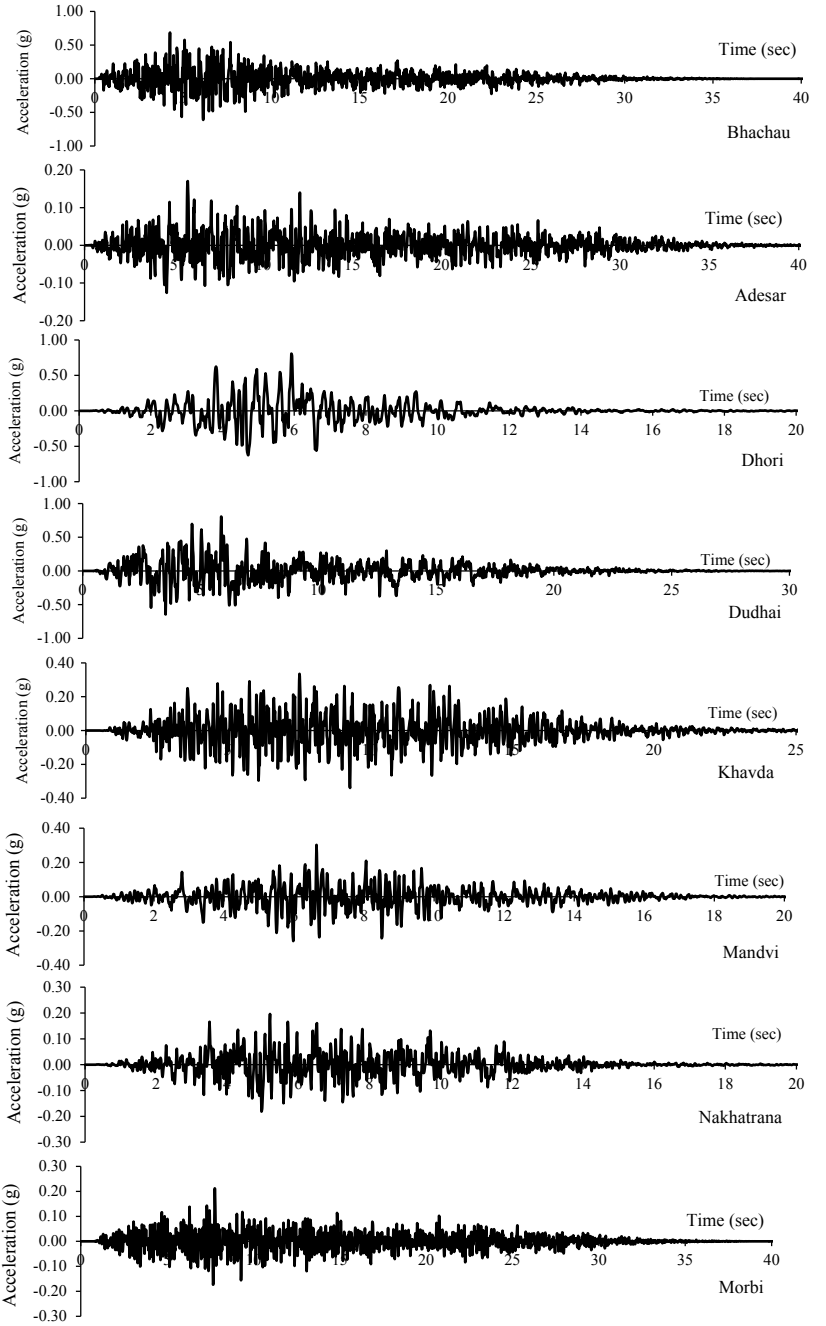

Fig. 2 Synthetic ground motions generated at surface-level using site amplification functions

Table 2 Results from nonlinear time-history analyses of URM walls using surface-level synthetic ground motions

S. No.	Station	Dist. (km)	MMI	PGA (g)	PGV (m/s)	T_p (s)	T_m (s)	Significant duration (s)	Disp. wall-1 (mm)	Disp. wall-2 (mm)
Sites in Zone 5 (IS1893:2016)—PSA(DBE) = 0.45 g										
1	Dudhai	15	X	0.74	0.87	0.21	0.55	12.81	7.5	16
2	Bhachau	19	X	0.64	0.54	0.10	0.31	18.08	7.5	16
3	Suvai	34	IX	0.38	0.32	0.22	0.35	21.38	7.5	16
4	Lakadia	36	IX	0.42	0.53	0.18	0.50	21.73	7.5	16
5	Rapar	46	IX	0.33	0.18	0.11	0.19	22.80	7.5	16
6	Dhori	49	X	0.74	0.63	0.26	0.40	5.92	7.5	16
7	Khavda	73	IX	0.35	0.18	0.15	0.23	12.24	7.5	16
8	Bela	77	IX	0.12	0.12	0.19	0.41	21.39	7.5	16
9	Adesar	78	VIII	0.15	0.13	0.19	0.38	22.88	7.5	16
10	Mandvi	111	VIII	0.24	0.17	0.14	0.26	9.26	7.5	16
11	Dayapur	141	VIII	0.13	0.09	0.16	0.29	7.80	7.5	13.6
12	Nakhtarana	155	VIII	0.20	0.16	0.13	0.33	8.31	7.5	16
13	Naliya	192	VIII	0.14	0.11	0.13	0.39	8.07	7.5	16
Sites in Zone 4 (IS1893:2016)—PSA(DBE) = 0.30 g										
14	Dwarka	183	VIII	0.03	0.03	0.25	0.46	9.95	3.4	3.99
15	Lalpur	122	VIII	0.09	0.05	0.11	0.18	13.67	6.11	6.19
16	Morbi	93	VIII	0.16	0.12	0.17	0.25	21.13	7.5	16
17	Radhanpur	148	VIII	0.06	0.07	0.30	0.49	24.33	7.5	10.81
18	Sipu	235	VIII	0.02	0.01	0.10	0.25	25.13	1.73	1.90

(continued)

Table 2 (continued)

S. No.	Station	Dist. (km)	MMI	PGA (g)	PGV (m/s)	T_p (s)	T_m (s)	Significant duration (s)	Disp. wall-1 (mm)	Disp. wall-2 (mm)
Sites in Zone 3 (IS1893:2016)—PSA(DBE) = 0.20 g										
19	Amreli	256	VII	0.017	0.006	0.08	0.13	20.51	2.91	1.04
20	Gandhinagar	248	VI	0.012	0.010	0.15	0.32	25.44	1.91	1.38
21	Jhagadia	354	VI	0.002	0.001	0.24	0.36	25.68	0.17	0.18
22	Junagadh	*235*	VII	0.019	0.010	0.09	0.17	18.45	1.71	1.37
23	Kadana	369	V	0.004	0.002	0.11	0.15	27.53	0.18	0.20
24	Kevadia	396	V	0.002	0.001	0.13	0.19	26.96	0.08	0.08
25	Rajkot	129	VII	0.065	0.074	0.45	0.54	19.16	7.5	9.80
26	Surendranagar	158	VII	0.047	0.041	0.21	0.36	23.34	5.21	5.41
27	Ukai	422	V	0.002	0.001	0.07	0.15	26.14	0.10	0.10
28	Una	280	V	0.009	0.005	0.17	0.24	19.61	1.41	0.63
29	Vadodara	321	V	0.004	0.003	0.22	0.32	25.61	0.33	0.35

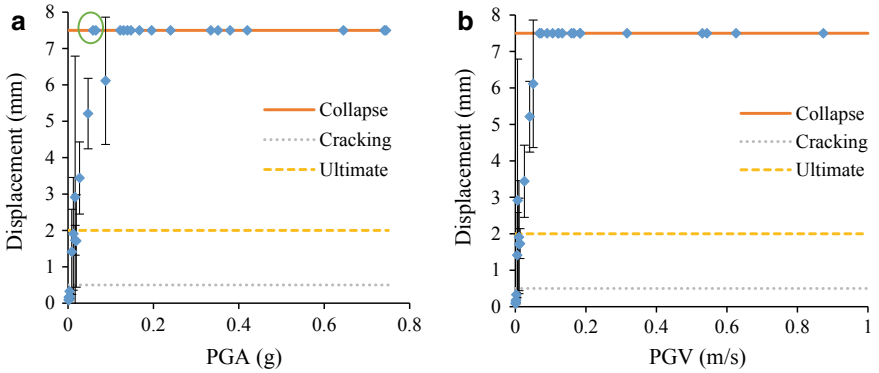

Fig. 3 **a** Displacement versus PGA (wall-1), **b** displacement versus PGV (wall-1)

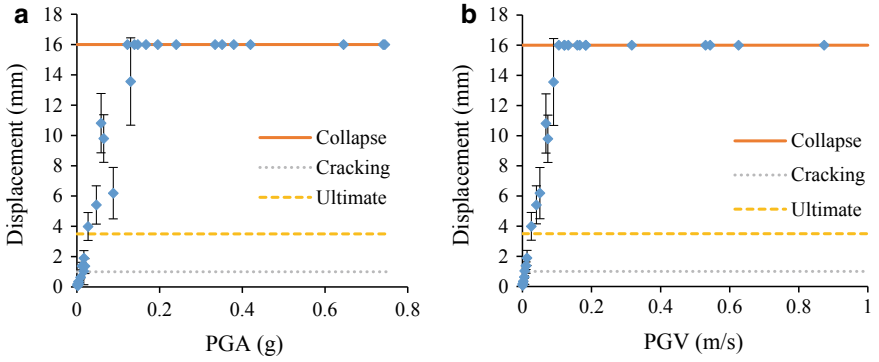

Fig. 4 **a** Displacement versus PGA (wall-2), **b** displacement versus PGV (wall-2)

collapse of the walls: this observation matches well with reconnaissance survey which reports catastrophic damage to low-rise masonry structures in this region. Figure 3 and Table 2 show that most towns in Seismic Zone 5 were assigned high MMI levels (X, IX and VIII) due to extensive damage observed to masonry structures [2, 5]. On the other extreme, ground motions from Zone 3 had very low PGA values and did not cause the collapse of the two URM walls. Some ground motions caused the walls to reach the cracking limit. This also corresponds well with data from reconnaissance surveys [2, 21] which show little or no damage to low-rise masonry construction in the 2001 Kutch earthquake. It is to be noted that the MMI levels for some towns in Zone 3 are higher due to high damage levels of mid-rise concrete buildings due to poor construction practices [2]. Ground motions in towns situated in Zone 4 caused the walls to exhibit displacements not exceeding the limit state of peak strength. Substantial damage to masonry structures was reported [5] in one particular town, Morbi, which is situated in Zone 4. In the current study, it is observed that surface-level ground motions in Morbi had high PGA values of 0.16 g, causing

both URM walls to collapse. The high PGAs observed in Morbi town are primarily due to site amplification [21].

The method of maximum likelihood has been recommended by several researchers [24–26] for fitting fragility curves for displacement data. The fitted fragility function is a lognormal cumulative distribution function, with a median, θ, and dispersion, β. Table 3 shows that for wall-1, the median values for cracking, ultimate strength and collapse are 0.01 g, 0.02 g and 0.06 g, respectively. For wall-2, the median values for cracking, ultimate strength and collapse are 0.01 g, 0.03 g and 0.12 g, respectively. In IS1893:2016, the peak spectral acceleration for design basis earthquake for seismic Zones 3, 4 and 5 are prescribed as 0.20 g, 0.30 g and 0.45 g, respectively. The median values are lower than expected seismic intensity indicating the high vulnerability of both walls.

Figure 5a, b show seismic demand fragility curves for both walls. The seismic intensity is represented by PGA. Figure 6 shows the fragility curves for the two walls, with PGV as the seismic intensity measure. The graphs provide a means to visually assess the vulnerability in terms of probability of exceedance of various limit states of the masonry shear walls, considering variability in demand. The damage state displacement thresholds were identified earlier, in Fig. 2, from the cyclic hysteric curves. The median values for achieving strength limit states for wall-1 and wall-2

Table 3 Fragility curves: median and dispersion

Damage state	Wall-1		Wall-2	
	Median, θ	Dispersion, β	Median, θ	Dispersion, β
Cracking	0.01	0.10	0.01	0.41
Strength	0.02	0.40	0.03	0.23
Collapse	0.06	0.52	0.12	0.26

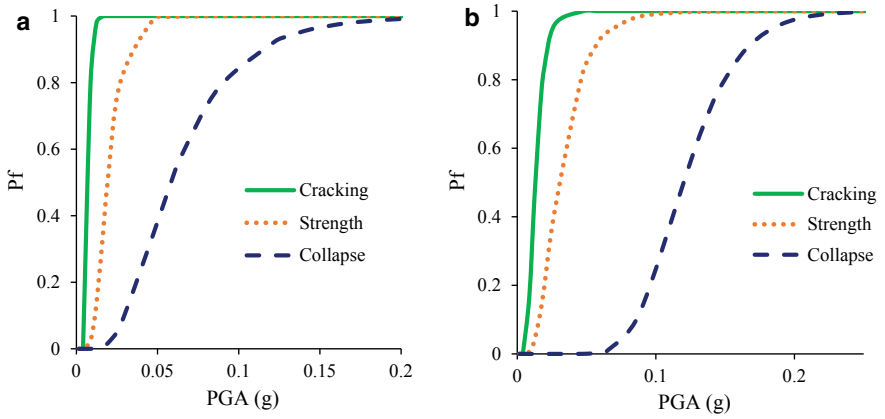

Fig. 5 **a** Seismic fragility curves (w.r.t. PGA) for wall-1, **b** seismic fragility curves (w.r.t. PGA) for wall-2

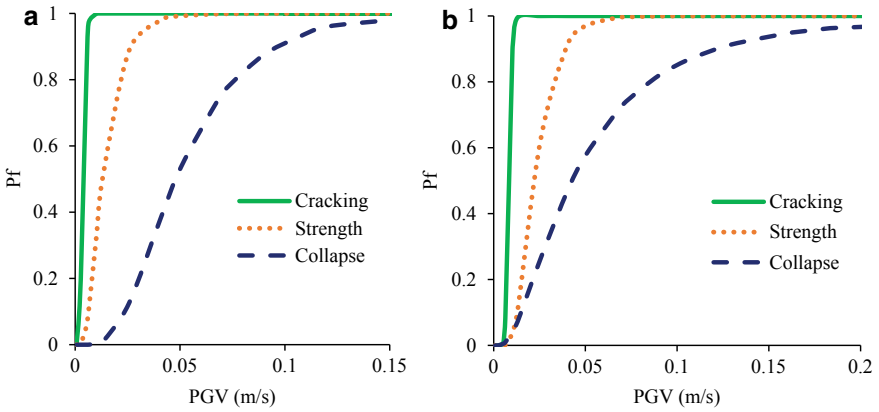

Fig. 6 **a** Seismic fragility curves (w.r.t. PGV) for wall-1, **b** seismic fragility curves (w.r.t. PGV) for wall-2

are 0.05 g and 0.1 g, respectively. The median values for achieving cracking limit for wall-1 and wall-2 are 0.01 g in both walls. The seismic fragility of the wall with higher axial load (wall-2) is only slightly lower than the wall with lower axial load (wall-1).

4 Anomalous Displacements/Outliers

In general, the wall displacement is observed to increase linearly with PGA, till collapse. However, it is observed that for two cases, Radhanpur (Zone 4) and Rajkot (Zone 3), the wall with lower axial load, differs slightly from the overall trend as the limit state of peak strength is reached at low PGA. These two outliers were shown, marked in Fig. 3. Figures 7 and 8 show velocity pulses from Radhanpur and Rajkot. Although the two records had low PGA, the occurrence of sharp velocity pulses triggered the collapse of the URM. The displacement time history in both cases shows that the velocity pulse imposed a high strength demand on the walls. Subsequently, there is a degradation in strength and stiffness of walls, leading to high displacements.

5 Summary and Conclusions

The 2001 Kutch earthquake was one of the most destructive intraplate earthquakes ever recorded. It had a moment magnitude of 7.6 and caused heavy damage to URM structures in the Kutch region. Unfortunately, no strong ground motions were

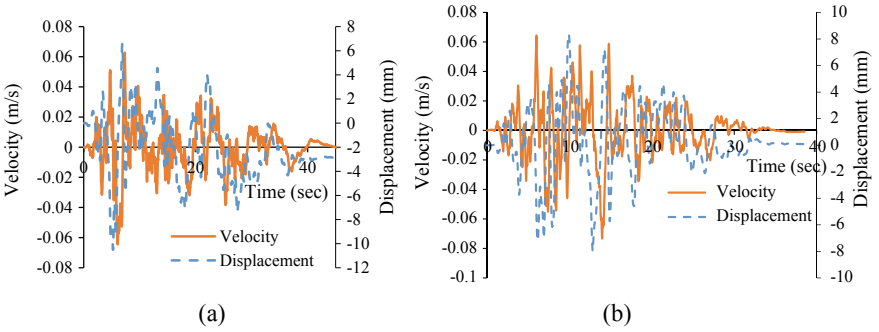

Fig. 7 **a** Radhanpur velocity pulse and displacement (wall-1), **b** Rajkot velocity pulse and displacement (wall-1)

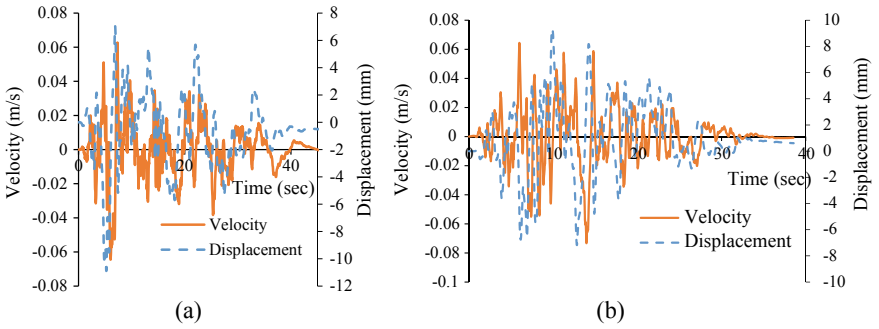

Fig. 8 **a** Radhanpur velocity pulse and displacement (wall-2), **b** Rajkot velocity pulse and displacement (wall-2)

recorded in this earthquake. Only PGA values from structural response recorders at thirteen sites are available. In this paper, nonlinear time-history analyses of URM walls are performed using surface-level synthetic ground motions. Characteristics of the ground motions such as PGA, PGV, frequency content and duration are tabulated. It is observed that ground motions have low values of predominant period. Such high-frequency ground motions could be particularly damaging to low-rise structures. A mechanics-based technique is used to develop the monotonic load envelope for two masonry shear walls. Using stress-based criteria, various displacement limit states are identified. Results from the dynamic analyses performed on calibrated hysteretic models were used to derive seismic fragility curves. Examination of the fragility curves indicates that the collapse limit state is reached for most towns in Zone 5, the highest seismic zone as per IS1893:2016. Most ground motions from Zone 5 have PGV values > 0.1 m/s and PGA values > 0.1 g and cause the walls to reach the collapse displacement levels. These results confirm satisfactorily with reconnaissance studies which report catastrophic damage to masonry structures in Zone 5, particularly in the epicentral region. Results from NTHA for towns situated in Seismic Zones 3 and 4

vary between no damage to collapse, which correlate well with post-earthquake field surveys carried out in these two zones, where varying levels of damage intensities were observed. The wall displacement is observed to vary linearly with PGA and PGV, until the collapse of the wall. Pulse ground motions from two distant sites, Radhanpur and Rajkot, had a destructive effect on the walls. It is concluded that URM structures with shear walls are highly vulnerable for expected ground motions in the Kutch region. Such URM structures existing in the Kutch region need to be upgraded to resist the expected level of seismic forces.

References

1. Nagamani, D., & Mandal, P. (2017). Estimation of earthquake source parameters in the Kachchh seismic zone, Gujarat, India, using three component S-wave spectra. *Journal of Earth System Science, 126*(5), 1–14.
2. Sinvhal, A., Bose, P. R., Prakash, V., Bose, A., Saraf, A. K., & Sinvhal, H. (2003). Isoseismals for the Kutch earthquake of 26th January 2001. *Journal of Earth System Science, 112*(3), 375–383.
3. Chopra, S., Kumar, D., & Rastogi, B. K. (2010). Estimation of strong ground motions for 2001 Bhuj (M_w 7.6), India earthquake. *Pure and Applied Geophysics, 167*(11), 1317–1330.
4. Rastogi, B. K., Gupta, H. K., Mandal, P., Satyanarayana, H. V. S., Kousalya, M., Raghavan, R., et al. (2001). The deadliest stable continental region earthquake occurred near Bhuj on 26 January 2001. *Journal of Seismology, 5*(4), 609–615.
5. Jagadish, K. (2003). Behaviour of masonry structures during the Bhuj earthquake of January 2001. *Journal of Earth System Science, 112*(3), 431–440.
6. WHE-PAGER Survey. (2007). Retrieved from http://www.world-housing.net/related-projects/whe-pager-project/about-this-project. Accessed July 2015.
7. Magenes, G., & Calvi, G. M. (1997). In-plane seismic response of brick masonry walls. *Earthquake Engineering and Structural Dynamics, 26,* 1091–1112.
8. Abrams, D. P. (1992). Strength and behavior of unreinforced masonry elements. In *Proceedings of the Tenth World Conference on Earthquake Engineering*, Madrid, Spain, July 19–24, 1992.
9. Vemuri, J., Ehteshamuddin, S., & Kolluru, S. (2018). Numerical simulation of soft brick unreinforced masonry walls subjected to lateral loads. *Cogent Engineering, 5*(1), 1551503.
10. Vemuri, J. P., & Kolluru, S. (2017). Seismic analysis of unreinforced masonry walls. *IDRiM Journal, 6*(2), 102–115.
11. Federal Emergency Management Agency (FEMA). (1999). *Evaluation of earthquake damaged concrete and masonry wall buildings: Technical resources* (FEMA P-307). Washington, DC.
12. Chopra, S., Kumar, D., Rastogi, B. K., Choudhury, P., & Yadav, R. B. S. (2012). Estimation of site amplification functions in Gujarat region, India. *Natural Hazards, 65*(2), 1135–1155.
13. Penelis, G. R. G. (2006). An efficient approach for pushover analysis of unreinforced masonry (URM) structures. *Journal of Earthquake Engineering, 10*(3), 359–379.
14. Vemuri, J., Ehteshamuddin, S., & Kolluru, S. V. L. (2018). Evaluation of seismic displacement demand for unreinforced masonry shear walls. *Cogent Engineering, 5*(1), 1480189.
15. Mann, W., & Muller, H. (1982). Failure of shear stressed masonry. An enlarged theory, tests and application to shear walls. *Proceedings of the British Ceramic Society, 30,* 223–235.
16. Anthoine, A., Magonette, G., & Magenes, G. (1995). Shear compression testing and analysis of brick masonry walls. In *Proceedings of the 10th European Conference on Earthquake Engineering*, August 28–September 02, 1994. Rotterdam: Balkema.
17. Magenes, G., & Calvi, G. M. (1992). Cyclic behaviour of brick masonry walls. In *Proceedings of the 10th World Conference on Earthquake Engineering*, Madrid, Spain, July 19–24, 1992.

18. BIS (Bureau of Indian Standards). (1991). *Handbook on masonry design and construction, SP:20*. New Delhi, India.
19. CSI (Computers and Structures Incorporated). (2012). *SAP2000 version 15, software*. Walnut Creek, California, USA.
20. Motazedian, D., & Atkinson, G. M. (2005). Stochastic finite-fault modelling based on dynamic corner frequency. *Bulletin Seismological Society of America, 95,* 995–1010.
21. Vemuri, J., Kolluru, S., & Chopra, S. (2018). Surface level synthetic ground motions for M7.6 2001 Gujarat earthquake. *Geosciences, 8*(12), 429.
22. Bureau of Indian Standards (BIS). (2016). *Indian Standard criteria for earthquake resistant design of structures: Part 1—General provisions and buildings, IS: 1893*. New Delhi, India.
23. Narayan, J. P., & Sharma, M. L. (2004). Effect of local geology on damage severity during Bhuj, India earthquake. In *Proceedings of the Thirteenth World Conference on Earthquake Engineering* (Paper No. 2042), Vancouver, Canada, August 1–4.
24. Baker, J. W., & Cornell, C. A. (2005). A vector-valued ground motion intensity measure consisting of spectral acceleration and epsilon. *Earthquake Engineering and Structural Dynamics, 34*(10), 1193–1217.
25. Cutfield, M. R., & Ma, Q. T. (2018). Solution strategies for three problems in empirical fragility curve derivation using the maximum likelihood method. *Journal of Earthquake Engineering, 22*(3), 435–453.
26. Straub, D., & Der Kiureghian, A. (2008). Improved seismic fragility modeling from empirical data. *Structural Safety, 30*(4), 320–336.